

Sequential Testing for Descriptor-Agnostic LiDAR Loop Closure in Repetitive Environments

Jaehyun Kim, Seungwon Choi, and Tae-Wan Kim

Abstract—We propose a descriptor-agnostic, multi-frame loop closure verification method that formulates LiDAR loop closure as a truncated Sequential Probability Ratio Test (SPRT). Instead of deciding from a single descriptor comparison or using fixed thresholds with late-stage Iterative Closest Point (ICP) vetting, the verifier accumulates a short temporal stream of descriptor similarities between a query and each candidate. It then issues an accept/reject decision adaptively once sufficient multi-frame evidence has been observed, according to user-specified Type-I/II error design targets. This precision-first policy is designed to suppress false positives in structurally repetitive indoor environments. We evaluate the verifier on a five-sequence library dataset, using a fixed retrieval front-end with several representative LiDAR global descriptors. Performance is assessed via segment-level K -hit precision–recall and absolute trajectory error (ATE) and relative pose error (RPE) after pose graph optimization. Across descriptors, the sequential verifier consistently improves precision and reduces the impact of aliased loops compared with single-frame and heuristic multi-frame baselines. Our implementation and dataset will be released at: https://github.com/wanderingcar/snu_library_dataset.

I. INTRODUCTION

Autonomous mobile robots (AMRs) are now deployed in factories, warehouses, and service environments to automate repetitive tasks and assist humans. Many commercial AMRs rely on LiDAR as a primary sensor for perception, localization, and mapping. In these systems, a consistent three-dimensional map of the environment is essential.

The quality of this LiDAR-based map depends strongly on accurate loop closure along the robot’s trajectory [1], [2]. LiDAR loop closure typically selects candidates by comparing the similarity of global descriptors between temporally separated point clouds. Numerous global descriptors have been proposed in recent years [3]–[8], and their reproducibility and efficiency have been demonstrated on public datasets [9]–[13]. As a result, global descriptors are now widely used for LiDAR-based place recognition and loop closure in modern SLAM systems. However, loop closure modules are often tuned to prioritize precision over recall: accumulated drift from missed loops grows gradually and can often be corrected once a valid loop is found, whereas a single false loop can severely distort the pose graph and corrupt the map, sometimes requiring re-mapping [14]–[17]. These risks are magnified in environments with strong structural repetition (e.g., warehouse racks, library stacks, industrial corridors) that induce severe perceptual aliasing, as illustrated in Fig.

The authors are with the Department of Naval Architecture and Ocean Engineering, Seoul National University, Seoul, South Korea (e-mail: jaedalong@snu.ac.kr; csw3575@snu.ac.kr; taewan@snu.ac.kr).



Fig. 1: The book repository at Seoul National University Library, showing repetitive shelving structures. The mobile robot, equipped with a 360-degree LiDAR, stereo camera, and IMU, was used to collect the dataset.

1 and Fig. 2. Despite the high potential risk of map corruption, robustly disambiguating structurally identical locations remains an open challenge. This suggests that there is still room for improvement in verification strategies designed to handle severe perceptual aliasing.

We propose a multi-frame loop *verification* method that suppresses false loop detections in highly repetitive environments. Unlike single-frame comparators that decide after one comparison, we cast loop closure as a truncated Sequential Probability Ratio Test (SPRT), i.e., a sequential test that accumulates evidence over short streams of descriptor similarities and issues an accept/reject decision only once the evidence is sufficient, according to user-specified design targets on false accepts and misses. We refer to this SPRT-based multi-frame verifier as *Seq-SPRT*. Our approach is descriptor-agnostic: it (i) generates top- M candidates using any global descriptor, (ii) aggregates multi-frame evidence via a sequential test, and (iii) marks only accepted hypotheses as loop closure constraints that can be passed to the pose graph back-end. We adopt a precision-first evaluation protocol tailored to aliasing-heavy environments, including a segment-level K -hit precision–recall metric that emphasizes short, temporally coherent match runs [14], [18] and post-PGO ATE/RPE. On a five-sequence library dataset dominated by repetitive shelving structures, the proposed verifier substantially reduces harmful false positives compared with

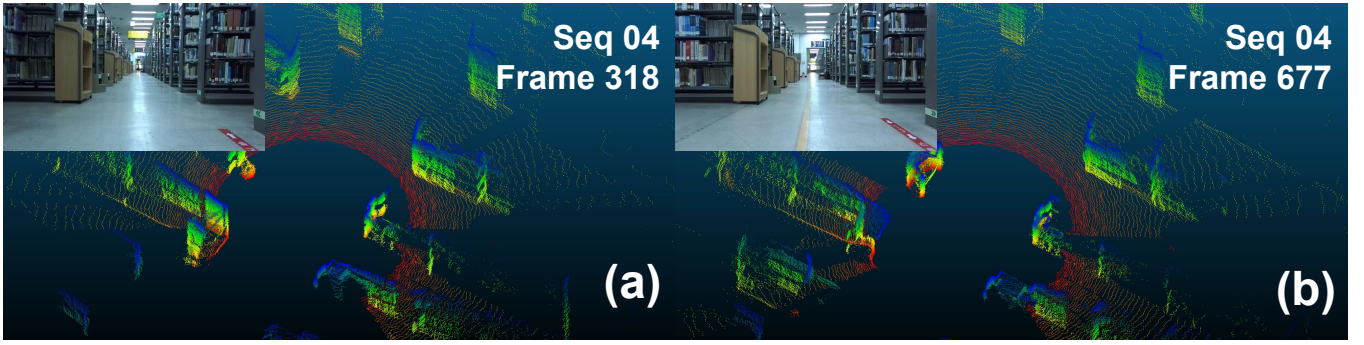


Fig. 2: Samples from the dataset. LiDAR scans and camera images for frame 318 (a) and frame 677 in Sequence 04. Although the viewpoints differ by more than 15 m, repeated structures induce nearly identical visual and geometric patterns.

single-frame and heuristic multi-frame baselines. Although multi-frame or sequence-aware LiDAR place-recognition has been explored, an explicit sequential decision policy that accumulates descriptor evidence and exposes Type-I/II error design targets has been less explored in LiDAR loop closure verification.

In summary, the contributions of our work are threefold:

- Seq-SPRT, a descriptor-agnostic, multi-frame loop verification policy that formulates loop closure as a sequential test over short streams of descriptor similarities, with user-specified design targets on false accepts and misses.
- An evaluation protocol for aliasing-heavy, repetitive-structure environments that emphasizes precision, combining segment-level K-hit precision-recall and post-PGO ATE/RPE.
- An experimental study on five library sequences demonstrating that (i) Seq-SPRT reduces harmful false positives compared with single-frame and heuristic multi-frame baselines, and (ii) Seq-SPRT is complementary to geometric verification: Seq-SPRT+ICP consistently yields the most stable pose graph optimization outcomes under strong aliasing.

II. RELATED WORK

LiDAR place recognition and loop closure are commonly built on global descriptors for efficient retrieval. Projection-based representations such as *Scan Context* and its variants have become widely used due to their simplicity and robustness in large-scale operation [3], [19]. In parallel, classical non-learning baselines include hand-crafted global descriptors and segment-level pipelines that trade compactness for distinctiveness and geometric robustness, e.g., *M2DP* and *SegMatch* [20], [21]. These methods primarily focus on improving the descriptor/retrieval stage, after which a separate verification step is typically applied.

Learning-based approaches instead encode point clouds into compact global embeddings optimized for discriminability under viewpoint and scene variation. Representative examples include *PointNetVLAD*, which aggregates point features using VLAD-style pooling, and *LPD-Net*, which

incorporates local structural cues to strengthen place recognition in challenging real-world settings [22], [23]. While learned embeddings can substantially improve retrieval quality, they usually require dedicated training and are more tightly coupled to the feature extractor than descriptor-agnostic verification layers.

To mitigate perceptual aliasing, recent work has incorporated additional cues such as overlap estimation and temporal structure. *OverlapNet* predicts scan overlap and relative yaw, providing richer verification signals than a single similarity score [24]. Transformer-based models further improve robustness: *OverlapTransformer* focuses on yaw-invariant matching with attention mechanisms, and *SeqOT* explicitly exploits short LiDAR sequences via spatial-temporal attention to stabilize recognition under viewpoint changes and repeated structures [25], [26]. These approaches typically embed temporal reasoning into the representation itself (often end-to-end), whereas our method preserves the descriptor extractor and instead introduces an explicit sequential *decision* policy on top of descriptor similarities.

Beyond descriptor matching, loop closure can also be strengthened by complementary verification cues, including geometric alignment (e.g., ICP-style checks), correspondence-based scoring using local features, or the integration of auxiliary signals when available. These approaches can be highly effective, but they may introduce additional computational cost, additional learned components, or tighter coupling to a specific SLAM back-end. In contrast, we focus on a lightweight verifier that operates directly on the native descriptor distance stream and can be attached to existing retrieval pipelines without retraining or modifying the front-end.

In vision-based place recognition, temporal consistency has long been exploited to improve robustness to aliasing and appearance changes. *SeqSLAM* demonstrated that sequence-level matching can outperform one-shot decisions in ambiguous settings, and probabilistic pipelines such as *FAB-MAP* exemplify decision-making beyond fixed similarity thresholds [18], [27]. Our work is conceptually aligned with this broader theme of accumulating evidence over time, but we target LiDAR loop *verification* and make the sequential decision rule explicit and tunable.

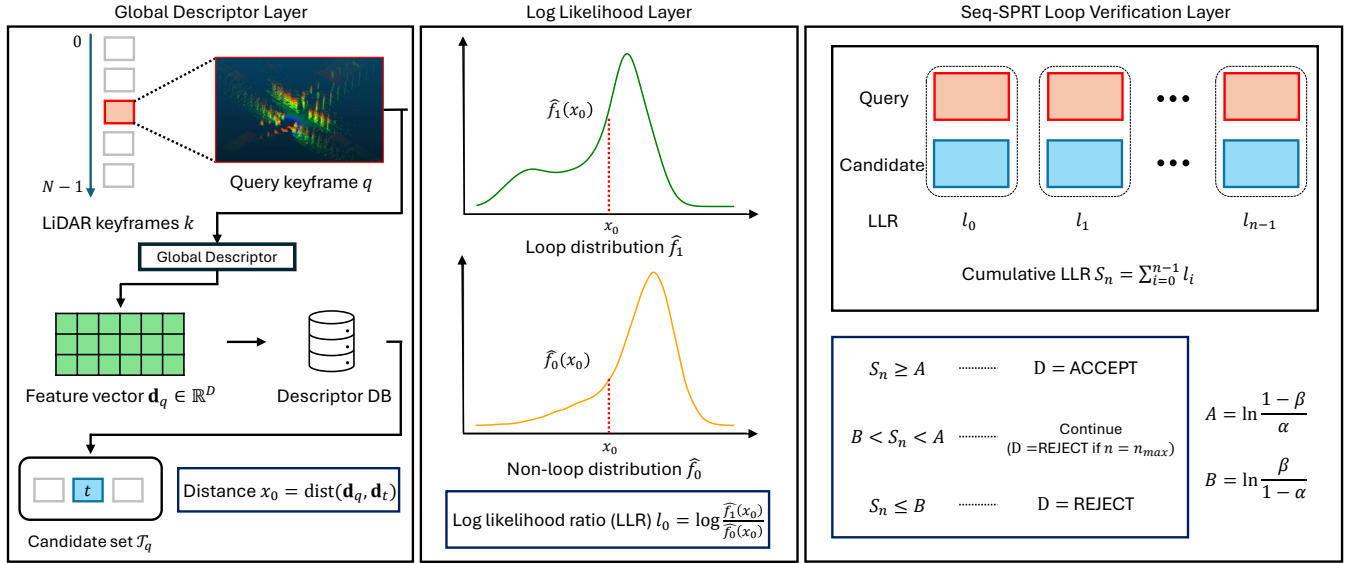


Fig. 3: Proposed Seq-SPRT loop-verification pipeline. Left: global-descriptor retrieval forms a candidate set for a query keyframe. Middle-right: descriptor distances are mapped to log-likelihood ratios using learned loop/non-loop distance densities and accumulated by a truncated SPRT to output **ACCEPT/REJECT**.

Sequential Probability Ratio Tests (SPRT) have been used to accelerate hypothesis verification in randomized model fitting (e.g., SPRT-style RANSAC verification) [28]. We differ in objective and setting: instead of accelerating geometric model checks, we formulate LiDAR loop closure verification itself as a truncated SPRT over short streams of descriptor distances. This yields an interpretable precision-first policy with user-specified Type-I/II design targets, while remaining descriptor-agnostic and computationally lightweight for aliasing-heavy indoor environments.

III. METHOD

A. Overview

We implement loop verification as a *descriptor-agnostic, multi-frame* sequential test attached to any retrieval front-end. We index LiDAR *keyframes* by $k \in \{0, \dots, N-1\}$. A global descriptor $g(\cdot)$ maps the scan at keyframe k to a feature vector $\mathbf{d}_k = g(\mathcal{P}_k) \in \mathbb{R}^D$, where \mathcal{P}_k denotes the pointcloud of keyframe index k . $\text{dist}(\cdot, \cdot)$ denotes the native distance for the chosen descriptor family (e.g., cosine, ℓ_1/ℓ_2 , Hamming).

For each query keyframe q , the retriever proposes a small candidate set $\mathcal{T}(q)$ in descriptor space. For each $(q, t) \in \{q\} \times \mathcal{T}(q)$, the verifier constructs a short near-diagonal stream of scalar distance observations $\{x_i\}$ by comparing descriptors from a small look-ahead window along both trajectories. These observations define a binary sequential hypothesis test, where hypothesis H_1 corresponds to a loop (match) and hypothesis H_0 corresponds to a non-loop (non-match).

From library sequences we fit one-dimensional empirical distance densities under each hypothesis, $\hat{f}_1(x)$ and $\hat{f}_0(x)$. At test time each observation contributes a per-step log-likelihood ratio (LLR), and the verifier accumulates evidence

over frames until it can confidently **ACCEPT** or **REJECT**. Concretely, we run a truncated Sequential Probability Ratio Test (SPRT) [29]–[32] on the cumulative LLR, with early stopping and a bounded horizon (n_{\min}, n_{\max}) to control latency. A global conflict-resolution step then selects an optimal non-overlapping subset of accepted loop segments before forwarding constraints to the SLAM back-end.

For each query-candidate pair (q, t) , the verifier chooses a stopping time τ and a terminal decision $D_\tau \in \{\text{ACCEPT}, \text{REJECT}\}$ from the prefix of observations $\{x_i\}_{i=0}^{\tau-1}$. We target Type-I/II error probabilities

$$\mathbb{P}_{H_0}(D_\tau = \text{ACCEPT}) \leq \alpha, \quad \mathbb{P}_{H_1}(D_\tau = \text{REJECT}) \leq \beta, \quad (1)$$

while keeping $\mathbb{E}[\tau]$ small under truncation. For a query q , the accepted loops are

$$\mathcal{A}(q) = \{t \in \mathcal{T}(q) : D_\tau(q, t) = \text{ACCEPT}\}. \quad (2)$$

This precision-first design constrains false accepts via (α, β) and allows the verifier to defer decisions until enough multi-frame evidence has accumulated.

B. Candidate Stream Construction

Unlike rigid diagonal verification which assumes constant velocity, we explicitly account for speed mismatch and temporal jitter. For each query-candidate pair (q, t) , we construct a descriptor distance stream:

$$x_i = \text{dist}(\mathbf{d}_{q+i}, \mathbf{d}_{t+k_i}), \quad k_i = \lfloor \nu \cdot i + \delta_i \rfloor, \quad (3)$$

where $i = 0, \dots, n-1$ is the look-ahead horizon. Here, ν accounts for velocity differences (adaptive stride) and $\delta_i \in [-\delta_{\max}, \delta_{\max}]$ handles local timing noise. At each step, the tracker greedily selects $\nu \in \mathcal{V}$ (a set of predefined velocity hypotheses) and $\delta_i \in [-\delta_{\max}, \delta_{\max}]$ to maximize

the instantaneous log-likelihood ratio (LLR) ℓ_i , representing match-vs-nonmatch evidence. This approach allows us to account for velocity mismatches and temporal jitter, improving robustness over simple raw similarity measures.

C. Evidence from Descriptor Distances

From the library sequences we collect scalar descriptor distances for loop (H_1) and non-loop (H_0) pairs and fit separate one-dimensional empirical distributions in the distance domain for each descriptor family. At test time, each observation x_i is mapped to a per-step log-likelihood ratio

$$\ell_i = \log \frac{\hat{f}_1(x_i)}{\hat{f}_0(x_i)}, \quad S_n = \sum_{i=0}^{n-1} \ell_i, \quad (4)$$

where \hat{f}_1 and \hat{f}_0 denote the learned distance distributions under loop and non-loop, respectively. We implement \hat{f}_c as simple 1D kernel density estimates evaluated on a tabulated grid with interpolation; in practice, any smooth 1D density model could be used here.

D. Sequential Test and Decision Policy

Given the cumulative LLR S_n in (4), the SPRT compares S_n to two thresholds A and B derived from the target error rates (α, β) :

$$A = \ln \frac{1 - \beta}{\alpha}, \quad B = \ln \frac{\beta}{1 - \alpha}. \quad (5)$$

Under standard assumptions (e.g., independent observations and correctly specified densities), SPRT is optimal in the sense of minimizing the expected sample number among tests satisfying the same error constraints [31], [32]. Since loop verification requires bounded latency, we use a truncated SPRT [32], [33]: at each step, we accept if $S_n \geq A$, reject if $S_n \leq B$, and otherwise continue sampling while $B < S_n < A$, subject to a maximum horizon n_{\max} . We enforce the minimum horizon n_{\min} only for acceptance to prevent premature false loops; rejection is allowed from the first sample when the accumulated evidence crosses the reject boundary. If no boundary is crossed by n_{\max} , the candidate is conservatively REJECTed.

To increase robustness to boundary noise, we also consider the maximum contiguous sub-segment of the LLR history:

$$S_{j,k} = \sum_{m=j}^k \ell_m, \quad S_{\max} = \max_{0 \leq j \leq k < n} S_{j,k}. \quad (6)$$

Upon acceptance we commit the segment attaining S_{\max} and apply a minimum accept-run constraint defined by the longest near-diagonal run (with a small gap tolerance) within this segment.

E. Global Conflict Resolution

Accepted segments from different candidates can overlap in their query or database index ranges. Before adding loop constraints to the pose graph, we keep only a non-overlapping subset: among all overlapping segments, we select the combination with the largest total score (segment

Algorithm 1 Seq-SPRT Loop Verification (overview)

Require: Query q , candidates $\mathcal{T}(q)$, densities \hat{f}_0, \hat{f}_1 , thresholds A, B , Horizons n_{\min}, n_{\max} .
Ensure: Accepted loop set $\mathcal{A}(q)$.

```

1:  $\mathcal{C} \leftarrow \emptyset$  // tentative accepted segments
2: for each  $t \in \mathcal{T}(q)$  do
3:    $S \leftarrow 0, \mathcal{H} \leftarrow []$  // cumulative LLR, per-step history
4:    $D \leftarrow \text{REJECT}$  // default: conservative
5:   for  $i = 0$  to  $n_{\max} - 1$  do
6:      $x_i \leftarrow \text{OBS}(q, t, i)$  // near-diagonal distance
7:      $\ell_i \leftarrow \log \frac{\hat{f}_1(x_i)}{\hat{f}_0(x_i)}$ 
8:      $S \leftarrow S + \ell_i$ ; append  $\ell_i$  to  $\mathcal{H}$ 
9:     if  $S \leq B$  then
10:       $D \leftarrow \text{REJECT}$  // early REJECT allowed
11:      break
12:     end if
13:     if  $i + 1 < n_{\min}$  then
14:       continue // defer decision until minimum evidence
15:     end if
16:     if  $S \geq A$  then
17:        $D \leftarrow \text{ACCEPT}$  // ACCEPT: enough evidence for loop
18:        $\mathcal{C} \leftarrow \mathcal{C} \cup \{\text{COMMIT}(q, t, \mathcal{H})\}$ 
19:       break
20:     end if
21:   end for // If no boundary crossed by  $n_{\max}$ : keep  $D = \text{REJECT}$ .
22: end for
23:  $\mathcal{A}(q) \leftarrow \text{RESOLVECONFLICT}(\mathcal{C})$  // get non-overlap best set
24: return  $\mathcal{A}(q)$ 

```

LLR plus a small length bonus) and discard weaker alternatives. The number of pending segments per window is small, so this selection can be done exactly with negligible overhead.

F. Practical Considerations

Each candidate requires at most $O(n_{\max})$ 1D density lookups and additions, and early stopping reduces average cost. Since per-step evidence can be weakly correlated, we treat (α, β) as design targets and rely on truncation.

In all experiments, we use a single set of SPRT hyperparameters across datasets and descriptor families. We fix the target error levels to $(\alpha, \beta) = (10^{-5}, 0.009)$, which yields thresholds $A \approx 11.5$ and $B \approx -4.71$ via (5). We set the minimum and maximum horizons to $(n_{\min}, n_{\max}) = (6, 13)$ frames. These values were selected on a held-out sequence and kept fixed for all evaluation runs. We empirically found that performance is stable under moderate variations of (α, β) and n_{\max} as long as α remains small (high precision) and n_{\max} is large enough to cover typical loop lengths.

IV. DATASET AND EVALUATION

A. SNU Library Dataset

Public LiDAR SLAM datasets with accurate ground-truth exist; however, datasets that are dominated by long, near-identical indoor aisles (e.g., shelf-and-corridor layouts) and

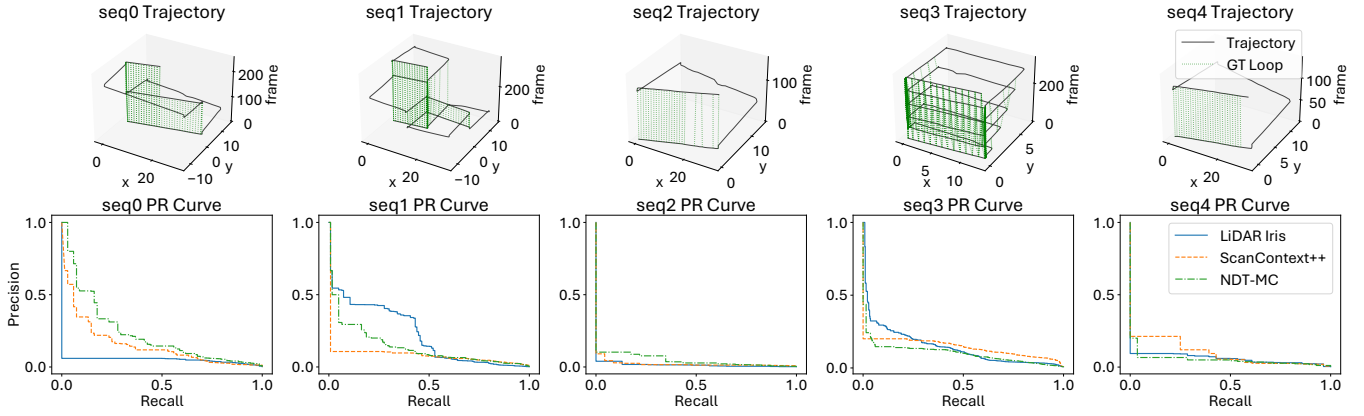


Fig. 4: Pseudo ground-truth trajectories (top) and single-frame precision-recall (PR) curves (bottom) for all five library sequences. The bottom row shows pairwise PR curves when each global descriptor (LiDAR Iris, ScanContext++, NDT-Map-Code) is used in the *Single* verification mode (one-shot decision, no multi-frame policy). Under strong structural aliasing, single-frame operation is confined to a very low-precision regime even before any multi-frame verification is applied.

are specifically tailored to stress-test perceptual aliasing for loop closure verification remain limited. We therefore collected a LiDAR-based indoor dataset in a library environment with highly repetitive shelf-and-corridor structures, which creates frequent perceptual ambiguity for global descriptors.

Data were recorded with a Clearpath Jackal equipped with an Ouster OS1-128 LiDAR, IMU, and a stereo camera; sensors were time-synchronized and extrinsically calibrated. We build pseudo ground-truth by running A-LOAM followed by global refinement [34]–[36]. The dataset contains five sequences dominated by repetitive shelf-and-corridor structures, inducing severe perceptual aliasing.

B. Evaluation Protocol on Library Sequences

We fix the retrieval stage and vary only the loop verification policy. All methods share the same loop-pair generation, retrieval/candidate gating, and pose graph optimization pipeline. Pseudo ground-truth trajectories are used to generate loop/non-loop labels for density estimation, and evaluation.

1) *Ground-truth*: Ground-truth (GT) loop pairs are obtained from the pseudo-GT trajectories by labeling two keyframes as a loop if their horizontal separation is below 0.5m and their relative rotation is within 12° in $SO(3)$. The translational threshold is smaller than the inter-aisle spacing and also absorbs keyframe discretization and residual pseudo-GT error. As a result, a GT loop corresponds to revisiting the same physical aisle cell rather than a neighboring shelf. The rotational threshold (12° geodesic distance in $SO(3)$, dominated by yaw for our ground robot) allows small heading variations while keeping a similar viewpoint, and lies in the same range as the distance/angle tolerances commonly used in laser-based place-recognition benchmarks [37], [38]. We additionally require a minimum temporal separation and discard near-duplicate pairs. Connected near-diagonal runs in the pairwise grid are then labeled as GT segments. All thresholds are fixed globally.

2) *Retrieval and candidate gating*: Per query, the retriever proposes a bounded set of database candidates. We exclude a short temporal neighborhood around the query, enforce an exclusivity span in database indices to avoid redundant neighbors, and apply light cluster gating in descriptor space. A fixed per-query budget then proceeds to verification.

3) *Sequential verification (ours)*: For each descriptor family, we apply the Seq-SPRT verifier (Sec. III). Loop/non-loop distance densities are learned once from the library sequences using 1D KDEs, and per-step log-likelihood ratios are accumulated along short near-diagonal streams under a truncated SPRT with a minimum-run guard. All SPRT-related hyperparameters are shared across descriptors and sequences and fixed globally (no per-sequence tuning).

4) *Descriptors under test*: The verifier is descriptor-agnostic; we instantiate it with three LiDAR global descriptors (LiDAR Iris [4], ScanContext++ [3], NDT-Map-Code (NDT-MC) [7]) used only for retrieval.

5) *Metrics and reporting*: We report metrics at three levels.

- 1) **Pair-wise precision/recall**. We report standard pair-wise precision/recall/F1 over loop pairs.
- 2) **Segment-level K -hit PR**. We additionally report a segment-level metric that discounts isolated hits and credits short, temporally coherent match runs [14], [18], [39].

We group predicted pairs into near-diagonal runs to form predicted segments $\hat{\mathcal{S}}$; GT segments are \mathcal{S} . Let $L_{\text{run}}(p, g)$ denote the longest run length between $p \in \hat{\mathcal{S}}$ and $g \in \mathcal{S}$ under a small gap tolerance. A predicted segment is a K -hit if

$$\max_{g \in \mathcal{S}} L_{\text{run}}(p, g) \geq K. \quad (7)$$

From these we compute P@Khit, R@Khit, and F1@Khit. We use $K = 5$ for all sequences and descriptors.

- 3) **Decision-tier (sequential) metrics.** Let τ be the stopping time in (1) and $D_\tau \in \{\text{ACCEPT}, \text{REJECT}\}$ the terminal decision. We report expected samples to decision conditioned on acceptance or rejection,

$$\begin{aligned} \text{ASN-acc} &= \mathbb{E}[\tau \mid D_\tau = \text{ACCEPT}], \\ \text{ASN-rej} &= \mathbb{E}[\tau \mid D_\tau = \text{REJECT}], \end{aligned} \quad (8)$$

and the detection delay for true accepts (frames),

$$\text{Delay} = \mathbb{E}[t_{\text{dec}} - t_{\text{birth}} \mid (q, t) \in \mathcal{G}, D_\tau = \text{ACCEPT}]. \quad (9)$$

All metrics are computed per sequence and averaged across sequences.

6) *Baselines:* All methods share the same retriever, GT, and back-end. For each baseline, we tune its hyperparameters on a held-out validation set to maximize $F1@Khit$. We compare six verification policies and our proposed Seq-SPRT:

- 1) **Single.** For each query-candidate pair (q, t) , threshold the native descriptor score once (no multi-frame aggregation).
- 2) **Single+ICP.** Apply Single to shortlist candidates, then run G-ICP for accepted pairs and discard those failing a fitness/inlier-ratio check.
- 3) **Single-LLR.** Convert a single distance x_0 to $\ell_0 = \log \frac{f_1(x_0)}{f_0(x_0)}$ using the learned 1D densities, then threshold ℓ_0 . This is a special one-step case of the sequential evidence model.
- 4) **N-of-M and FixedBatch.** Given M distances $\{x_i\}_{i=0}^{M-1}$ along the stream, N-of-M accepts if at least N per-step LLRs exceed a threshold; FixedBatch thresholds the average LLR.
- 5) **Ours (Seq-SPRT).** Truncated SPRT-based multi-frame verifier with early stopping.
- 6) **Ours (Seq-SPRT+ICP).** Run Seq-SPRT and apply G-ICP only to hypotheses accepted by Seq-SPRT. Pairs failing the ICP fitness/inlier-ratio check are discarded; surviving pairs are used as loop constraints.

All baselines and our method use the same per-query candidate budget and globally fixed hyperparameters per descriptor family.

V. EXPERIMENTS

A. Experimental Setup

We evaluate the verification policies on the five library sequences using the dataset, ground-truth, and metrics defined in Sec. IV. We instantiate three representative LiDAR global descriptor families (LiDAR Iris, ScanContext++, NDT-MC) and six verification policies (Single, Single+ICP, Single-LLR, N-of-M, FixedBatch) plus our Seq-SPRT and Seq-SPRT+ICP. For Seq-SPRT we reuse the descriptor-specific distance distributions and global SPRT hyperparameters introduced in Sec. III, calibrated once on the library dataset and then kept fixed for all runs.

B. Loop Verification Performance on Library Sequences

1) *Segment-level K -hit metrics:* The left block of Table I reports segment-level K -hit metrics. Single and Single-LLR can achieve moderate $R@Khit$ (up to 0.513), but $P@Khit$ remains low ($P@Khit \leq 0.107$), indicating many spurious segments under aliasing. Heuristic multi-frame rules improve $F1@Khit$ for LiDAR Iris and NDT-MC (0.241 and 0.224), but do not consistently help ScanContext++ (0.095/0.145 for N-of-M/FixedBatch). Seq-SPRT yields the highest $F1@Khit$ for ScanContext++ and NDT-MC (0.493 and 0.268) and is close to the best for LiDAR Iris (0.237 vs. 0.241). Single+ICP shifts the pair-wise operating point, but segment-level $F1@Khit$ remains ≤ 0.096 . When combined with ICP, Seq-SPRT+ICP further increases segment-level precision and $F1$ across all descriptors, indicating that sequential evidence accumulation and geometric verification are strongly complementary under aliasing-heavy repetition.

Overall, Seq-SPRT achieves the best $F1@Khit$ on two descriptors and remains close to the best on the third, making it a robust descriptor-only choice for temporally coherent loop segments under aliasing.

2) *Pair-wise precision/recall:* The middle block of Table I reports pair-wise precision/recall/ $F1$. Single+ICP increases precision via geometric verification, but its operating point is still determined by one-shot descriptor gating. Seq-SPRT deliberately operates in a conservative, precision-first regime using multi-frame statistical evidence, and its accepted hypotheses can be further purified by ICP. Accordingly, Seq-SPRT+ICP achieves the highest pair-wise precision across descriptors in Table I, while maintaining a conservative acceptance policy designed to avoid harmful false constraints. Seq-SPRT provides the highest pair-wise precision among descriptor-only policies, and its conservative accept decisions are compatible with downstream geometric refinement when available.

C. Decision-tier Behavior

To better understand how Seq-SPRT behaves as a sequential decision mechanism, we analyze its stopping times and empirical decision-level error ratios. Table II reports the expected number of samples to decision for accepted and rejected hypotheses (ASN-acc , ASN-rej), the average detection delay in frames (Delay).

We apply the minimum horizon n_{\min} only to *acceptance* (minimum-evidence guard), while allowing *early rejection* as soon as the reject boundary is crossed. Accordingly, accepted loops are typically confirmed within a short window (ASN-acc between 5 and 9 across descriptors), and the measured delay closely tracks this stopping time (approximately $\text{Delay} \approx \text{ASN-acc} - 1$ in frames). Rejection behavior is descriptor-dependent: for LiDAR Iris and NDT-MC, many non-loop candidates accumulate negative evidence quickly, yielding early rejections ($\text{ASN-rej} = 2.57$ and 3.35), whereas ScanContext++ exhibits more ambiguous non-loop streams and thus requires more samples on average before crossing the reject boundary ($\text{ASN-rej} = 11.78$), still below the truncation horizon.

TABLE I: Summary of loop-verification performance on the library dataset (mean over five sequences). Segment-level K -hit metrics, pair-wise metrics, and post-PGO trajectory errors are reported for each descriptor and verification policy.

Descriptor	Policy	Segment-level K -hit			Pair-wise			PGO Result (RMSE)	
		P@Khit	R@Khit	F1@Khit	Prec	Rec	F1	ATE [m] ↓	RPE [m] ↓
LiDAR Iris	Single	0.037	0.513	0.067	0.241	0.379	0.267	11.39	1.46
	Single+ICP	0.054	0.513	0.096	0.435	0.355	0.386	5.42	0.31
	Single-LLR	0.034	0.433	0.063	0.276	0.302	0.280	9.54	0.24
	N-of-M	0.116	0.617	0.191	0.163	0.042	0.066	9.42	0.21
	FixedBatch	0.156	0.617	0.241	0.234	0.042	0.070	7.45	0.09
	Seq-SPRT (Ours)	0.156	0.590	0.237	0.326	0.056	0.094	4.90	0.08
	Seq-SPRT+ICP (Ours)	0.250	0.540	0.337	0.454	0.043	0.079	4.27	0.10
ScanContext++	Single	0.107	0.407	0.169	0.431	0.217	0.285	8.16	0.24
	Single+ICP	0.063	0.207	0.095	0.686	0.215	0.320	1.81	0.10
	Single-LLR	0.083	0.487	0.141	0.348	0.250	0.288	8.53	0.34
	N-of-M	0.053	0.713	0.095	0.084	0.048	0.057	11.64	0.41
	FixedBatch	0.085	0.593	0.145	0.128	0.041	0.060	10.84	0.17
	Seq-SPRT (Ours)	0.387	0.907	0.493	0.548	0.071	0.122	5.07	0.14
	Seq-SPRT+ICP (Ours)	0.463	0.807	0.565	0.717	0.064	0.118	1.13	0.06
NDT-MC	Single	0.016	0.220	0.028	0.156	0.242	0.174	11.56	1.40
	Single+ICP	0.019	0.220	0.035	0.298	0.231	0.257	6.42	0.37
	Single-LLR	0.011	0.193	0.020	0.175	0.265	0.204	10.87	0.68
	N-of-M	0.121	0.713	0.203	0.177	0.049	0.076	8.41	0.40
	FixedBatch	0.135	0.713	0.224	0.192	0.049	0.077	9.11	0.25
	Seq-SPRT (Ours)	0.163	0.807	0.268	0.280	0.070	0.110	6.47	0.22
	Seq-SPRT+ICP (Ours)	0.307	0.807	0.442	0.428	0.059	0.104	3.26	0.06

TABLE II: Decision-tier metrics for Seq-SPRT averaged over five library sequences. ASN: expected number of samples to decision; Delay is measured in frames.

Metric	LiDAR Iris	ScanContext++	NDT-MC
ASN-acc	5.38	8.59	6.41
ASN-rej	2.57	11.78	3.35
Delay [frames]	4.58	7.59	5.41

D. Impact on Pose Graph Optimization

The library dataset is intentionally aliasing-heavy yet relatively compact: pure odometry already yields low drift (odometry-only ATE ≈ 0.22 m), leaving limited headroom for improvements from additional correct loop closures. In this regime, post-PGO ATE/RPE primarily act as a robustness stress-test: a small number of aliased loop constraints can dominate pose graph optimization (PGO) and severely distort the map. Single can degrade PGO (e.g., LiDAR Iris 11.39 m/1.46 m), and heuristic multi-frame rules are mixed (e.g., ScanContext++ N-of-M 11.64 m/0.41 m). With geometric verification, Seq-SPRT+ICP achieves the lowest post-PGO errors across all three descriptors, demonstrating that sequential verification is an effective pre-filter that makes ICP significantly more reliable in repetitive environments. Compared with the conventional Single+ICP pipeline, Seq-SPRT+ICP consistently reduces the impact of aliased constraints and yields the most stable pose graph optimization outcomes.

VI. CONCLUSION

We addressed loop closure verification for LiDAR SLAM in structurally repetitive environments, where perceptual aliasing severely challenges global-descriptor-based meth-

ods. Instead of deciding from a single comparison, we cast loop verification as a descriptor-agnostic, multi-frame sequential test: loop/non-loop distance densities are learned from data, log-likelihood ratios are accumulated along short near-diagonal streams, and a truncated SPRT with decide-delay-reject outcomes implements precision-first control via (α, β) design targets.

On a five-sequence library dataset dominated by repetitive shelves and narrow aisles, the proposed Seq-SPRT policy improves segment-level K -hit precision and F1 over single-frame baselines and remains competitive with heuristic multi-frame voting schemes, while offering conservative and interpretable decision behavior. When integrated into a pose graph optimization pipeline on our library sequences, Seq-SPRT reduces the impact of aliased loops and tends to move the resulting trajectories toward the pseudo ground-truth compared with the single-frame and heuristic multi-frame baselines.

Moreover, the proposed sequential verifier is complementary to geometric alignment: the hybrid Seq-SPRT+ICP mode consistently produced the most robust pose graph results in our aliasing-heavy library dataset, supporting the role of sequential testing as a precision-first front-end that strengthens downstream geometric verification.

Future work includes cross-dataset evaluation with disjoint training/test environments, joint modeling of multiple cues (e.g., LiDAR plus visual or semantic information), and adaptive policies that adjust (α, β) or truncation horizons online based on scene context and computational budget.

REFERENCES

- [1] S. Thrun, W. Burgard, and D. Fox, *Probabilistic Robotics*. Cambridge, MA, USA: MIT Press, 2005.

- [2] C. Cadena, L. Carlone, H. Carrillo, Y. Latif, D. Scaramuzza, J. Neira, I. Reid, and J. J. Leonard, "Past, present, and future of simultaneous localization and mapping: Toward the robust-perception age," *IEEE Transactions on Robotics*, vol. 32, no. 6, pp. 1309–1332, 2016.
- [3] G. Kim, S. Choi, and A. Kim, "Scan Context++: Structural place recognition robust to rotation and lateral variations in urban environments," *IEEE Trans. Robot.*, vol. 38, no. 3, pp. 1856–1874, 2022.
- [4] Y. Wang, Z. Sun, C.-Z. Xu, S. E. Sarma, J. Yang, and H. Kong, "LiDAR Iris for loop-closure detection," in *Proc. IEEE/RSJ Int. Conf. on Intelligent Robots and Systems (IROS)*, 2020, pp. 5769–5775.
- [5] Y. Fan, X. Du, L. Luo, and J. Shen, "FreSCo: Frequency-domain Scan Context for robust LiDAR-based place recognition with translation and rotation invariance," in *Proc. Int. Conf. on Control, Automation, Robotics and Vision (ICARCV)*, 2022, pp. 606–611.
- [6] C. Yuan, J. Lin, Z. Liu, H. Wei, X. Hong, and F. Zhang, "BTC: A binary and triangle combined descriptor for 3d place recognition," *IEEE Trans. Robot.*, vol. 40, no. 6, pp. 1580–1599, 2024.
- [7] L. Liao, W. Yan, L. Sun, X. Bai, Z. You *et al.*, "NDT-Map-Code: A 3d global descriptor for real-time loop closure detection in lidar slam," *IEEE Trans. Instrum. Meas.*, vol. 73, no. 8502115, pp. 1–13, 2024.
- [8] S. Gupta, I. Vizzo, J. Behley, and C. Stachniss, "Effectively detecting loop closures using point cloud density maps," *IEEE Robotics and Automation Letters (RA-L)*, vol. 8, no. 2, pp. 1029–1036, 2023.
- [9] A. Geiger, P. Lenz, C. Stiller, and R. Urtasun, "Are we ready for autonomous driving? the kitti vision benchmark suite," in *Proceedings of the IEEE Conference on Computer Vision and Pattern Recognition (CVPR)*, 2012, pp. 3354–3361.
- [10] P. Wenzel, L. Stumberg, M. Schönbein, and D. Cremers, "4Seasons: A cross-season dataset for multi-weather SLAM in autonomous driving," 2020.
- [11] G. Kim and A. Kim, "MulRan: Multimodal range dataset for urban place recognition," in *IEEE International Conference on Robotics and Automation (ICRA)*, 2020, pp. 6246–6253.
- [12] M. Ramezani, D. Wisth, M. Gadd, D. De Martini, P. Newman, I. Posner, and J. J. Leonard, "The newer college dataset: Handheld LiDAR, airborne and ground truth data for research in autonomous navigation," in *IEEE International Conference on Robotics and Automation (ICRA)*, 2020, pp. 5839–5845.
- [13] W. Maddern, G. Pascoe, C. Linegar, and P. Newman, "1 year, 1000 km: The Oxford RobotCar Dataset," *The International Journal of Robotics Research*, vol. 36, no. 1, pp. 3–15, 2017.
- [14] K. L. Ho and P. Newman, "Detecting loop closure with scene sequences," *International Journal of Computer Vision*, vol. 74, no. 3, pp. 261–286, 2007.
- [15] Y. Latif, C. C. Lerma, and J. Neira, "Robust loop closing over time," in *Proceedings of Robotics: Science and Systems*, Sydney, Australia, July 2012.
- [16] N. Sünderhauf and P. Protzel, "Switchable constraints vs. max-mixture models vs. RRR – a comparison of three approaches to robust pose graph SLAM," in *Proceedings of the IEEE International Conference on Robotics and Automation (ICRA)*, 2013, pp. 5198–5203.
- [17] S. B. Nashed, "A brief survey of loop closure detection: A case for rethinking evaluation of intelligent systems," in *NeurIPS 2020 Workshop on Machine Learning Retrospectives, Surveys & Meta-Analyses (ML-RSA)*, 2020.
- [18] M. J. Milford and G. F. Wyeth, "Seqslam: Visual route-based navigation for sunny summer days and stormy winter nights," in *Proc. IEEE Intl. Conf. on Robotics and Automation (ICRA)*, 2012, pp. 1643–1649.
- [19] G. Kim and A. Kim, "Scan Context: Egocentric spatial descriptor for place recognition within 3d point cloud map," in *Proc. IEEE/RSJ Int. Conf. on Intelligent Robots and Systems (IROS)*, 2018, pp. 4802–4809.
- [20] L. He, X. Wang, and H. Zhang, "M2dp: A novel 3d point cloud descriptor and its application in loop closure detection," in *Proc. IEEE/RSJ Intl. Conf. on Intelligent Robots and Systems (IROS)*, 2016.
- [21] R. Dubé, D. Dugas, E. Stumm, J. Nieto, R. Siegwart, and C. Cadena, "Segmatch: Segment based place recognition in 3d point clouds," in *Proc. IEEE Intl. Conf. on Robotics and Automation (ICRA)*, 2017, pp. 5266–5272.
- [22] M. A. Uy and G. H. Lee, "Pointnetvlad: Deep point cloud based retrieval for large-scale place recognition," in *Proc. IEEE/CVF Conf. on Computer Vision and Pattern Recognition (CVPR)*, 2018, pp. 4470–4479.
- [23] Z. Liu, S. Zhou, C. Suo, P. Yin, W. Chen, H. Wang, H. Li, and Y.-H. Liu, "Lpd-net: 3d point cloud learning for large-scale place recognition and environment analysis," in *Proc. IEEE/CVF Intl. Conf. on Computer Vision (ICCV)*, 2019.
- [24] X. Chen, T. Labe, A. Milioto, T. Röhling, J. Behley, and C. Stachniss, "Overlapnet: A siamese network for computing lidar scan similarity with applications to loop closing and localization," *Autonomous Robots*, vol. 46, no. 1, pp. 61–81, 2022.
- [25] J. Ma, J. Zhang, J. Xu, R. Ai, W. Gu, and X. Chen, "Overlaptransformer: An efficient and yaw-angle-invariant transformer network for lidar-based place recognition," *IEEE Robotics and Automation Letters*, vol. 7, no. 3, pp. 6958–6965, 2022.
- [26] J. Ma, X. Chen, J. Xu, and G. Xiong, "Seqot: A spatial-temporal transformer network for place recognition using sequential lidar data," *IEEE Transactions on Industrial Electronics*, vol. 70, no. 8, pp. 8225–8234, 2023.
- [27] M. Cummins and P. Newman, "Fab-map: Probabilistic localization and mapping in the space of appearance," *The International Journal of Robotics Research*, vol. 27, no. 6, pp. 647–665, 2008.
- [28] J. Matas and O. Chum, "Randomized ransac with sequential probability ratio test," in *Proceedings of the 10th IEEE International Conference on Computer Vision (ICCV)*, 2005.
- [29] A. Wald, "Sequential tests of statistical hypotheses," *Annals of Mathematical Statistics*, vol. 16, no. 2, pp. 117–186, 1945.
- [30] —, *Sequential Analysis*. New York: John Wiley & Sons, 1947.
- [31] A. Wald and J. Wolfowitz, "Optimum character of the sequential probability ratio test," *Annals of Mathematical Statistics*, vol. 19, no. 3, pp. 326–339, 1948.
- [32] D. Siegmund, *Sequential Analysis: Tests and Confidence Intervals*, ser. Springer Series in Statistics. New York: Springer, 1985.
- [33] A. G. Tartakovsky, I. V. Nikiforov, and M. Basseville, *Sequential Analysis: Hypothesis Testing and Changepoint Detection*. Boca Raton, FL: CRC Press, 2014.
- [34] J. Zhang and S. Singh, "LOAM: Lidar odometry and mapping in real-time," in *Proceedings of Robotics: Science and Systems (RSS)*, 2014.
- [35] X. Liu, Z. Liu, F. Kong, and F. Zhang, "Large-scale lidar consistent mapping using hierarchical lidar bundle adjustment," *IEEE Robotics and Automation Letters*, vol. 8, no. 3, pp. 1523–1530, 2023.
- [36] Z. Liu, X. Liu, and F. Zhang, "Efficient and consistent bundle adjustment on lidar point clouds," *IEEE Transactions on Robotics*, vol. 39, no. 6, pp. 4366–4386, 2023.
- [37] G. D. Tipaldi, M. Braun, and K. O. Arras, "Flirt: Interest regions for 2d range data with applications to robot navigation," in *Experimental Robotics: The 12th International Symposium on Experimental Robotics*. Springer, pp. 695–710.
- [38] M. Bosse and R. Zlot, "Place recognition using regional point descriptors for 3d mapping," in *Field and Service Robotics: Results of the 7th International Conference*. Springer, 2010, pp. 195–204.
- [39] R. Mur-Artal, J. M. M. Montiel, and J. D. Tardos, "Orb-slam: A versatile and accurate monocular slam system," *IEEE transactions on robotics*, vol. 31, no. 5, pp. 1147–1163, 2015.